

## Article

# Evolution of a Late Miocene Deep-Water Depositional System in the Southern Taranaki Basin, New Zealand

Clayton Silver \* and Heather Bedle 

School of Geosciences, University of Oklahoma, Norman, OK 73069, USA; hbedle@ou.edu

\* Correspondence: clayton.j.silver-1@ou.edu

**Abstract:** A long-standing problem in the understanding of deep-water turbidite reservoirs relates to how the three-dimensional evolution of deep-water channel systems evolve in response to channel filling on spatiotemporal scales, and how depositional environments affect channel architecture. The 3-D structure and temporal evolution of late Miocene deep-water channel complexes in the southern Taranaki Basin, New Zealand is investigated, and the geometry, distribution, and stacking patterns of the channel complexes are analyzed. Two recently acquired 3-D seismic datasets, the Pipeline-3D (proximal) and Hector-3D (distal) are analyzed. These surveys provide detailed imaging of late Miocene deep-water channel systems, allowing for the assessment of the intricate geometry and seismic geomorphology of the systems. Seismic attributes resolve the channel bodies and the associated architectural elements. Spectral decomposition, amplitude curvature, and coherence attributes reveal NW-trending straight to low-sinuosity channels and less prominent NE-trending high-sinuosity feeder channels. Stratal slices across the seismic datasets better characterize the architectural elements. The mapped turbidite systems transition from low-sinuosity to meandering high-sinuosity patterns, likely caused by a change in the shelf-slope gradient due to localized structural relief. Stacking facies patterns within the channel systems reveal the temporal variation from a depositional environment characterized by sediment bypass to vertically aggrading channel systems.

**Keywords:** seismic analysis; attributes; deep-water channel; channel evolution



**Citation:** Silver, C.; Bedle, H. Evolution of a Late Miocene Deep-Water Depositional System in the Southern Taranaki Basin, New Zealand. *Geosciences* **2021**, *11*, 329. <https://doi.org/10.3390/geosciences11080329>

Academic Editors: Piotr Krzywiec, Marco Roveri and Jesus Martinez-Frias

Received: 11 May 2021  
Accepted: 31 July 2021  
Published: 3 August 2021

**Publisher's Note:** MDPI stays neutral with regard to jurisdictional claims in published maps and institutional affiliations.



**Copyright:** © 2021 by the authors. Licensee MDPI, Basel, Switzerland. This article is an open access article distributed under the terms and conditions of the Creative Commons Attribution (CC BY) license (<https://creativecommons.org/licenses/by/4.0/>).

## 1. Introduction

The Taranaki Basin is located off the west coast of the North Island of New Zealand and covers an area of approximately 330,000 km<sup>2</sup>. The majority of the Taranaki Basin is located offshore, and water depths range from 120 m on the shelf to over 3300 m in the deepest part. During the Neogene, a second-order regression enhanced widespread sediment transport resulting in the formation of complex shelf-to-slope channel systems. On the western coast of the North Island, seismic-scale outcrops of deep-water channels within the Late-Miocene Mount Messenger Formation have been previously studied [1–3]. The aim of this study is to observe and understand the spatial and temporal evolution of the southern equivalents of the Mount Messenger Formation within the Southern Taranaki Basin through integrating seismic attribute analysis and seismic geomorphology techniques. Two 3-D seismic datasets were utilized to visualize the depositional system and intersecting 2-D seismic lines were used to correlate the two surveys. Three wells were used to constrain the interpretations from seismic data.

In this region of the Southern Taranaki Basin (Figure 1A,B), channel complexes range from 250 m to two kilometers width, from high to low sinuosity, and from heavily-incised to laterally stacking, revealing a complex depositional system [4]. As the Taranaki Basin is New Zealand's only hydrocarbon producing basin to date [5], much research has been performed regarding the tectonic and stratigraphic history of the region to better characterize reservoirs within the Mt. Messenger Formation [1,6–9]. The observed siliciclastic, deep-water channels in this study region were formed in response to basin subsidence and uplift in the hinterland [10], and primarily transported fine-grained sediments [11].

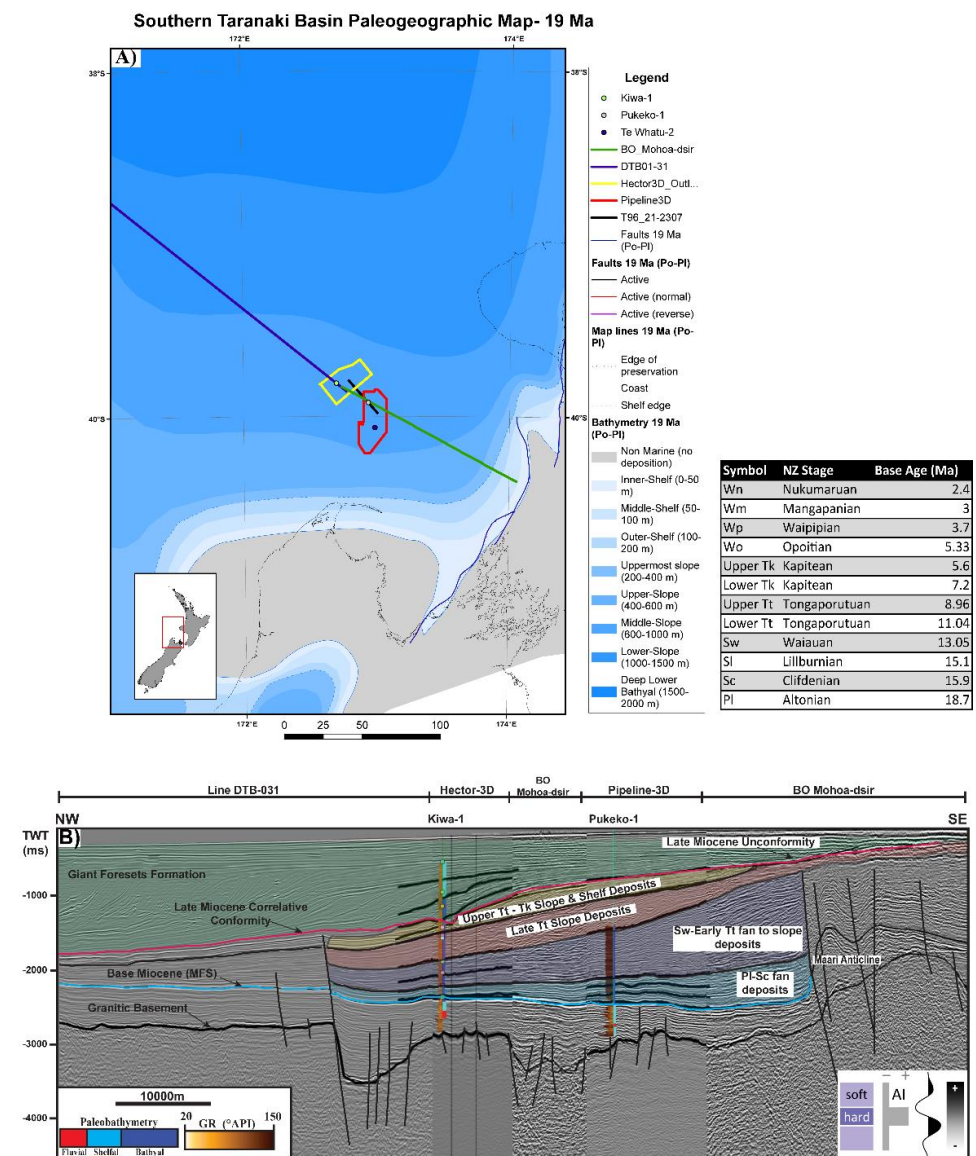


**Figure 1.** (A): A 19 Ma Paleogeographic map of the southern Taranaki Basin with the seismic surveys and well locations used in this study overlain. Modified after Arnot and Bland (2016) [12]. (B): regional composite 2D seismic section through the southern Taranaki Basin with depositional environment interpretations overlain. A summary of the Taranaki Basin Timescale abbreviations is provided in the table.

To understand the larger scale depositional architecture of this late-Miocene deep-water system, it was necessary to analyze two recent 3-D seismic surveys: The Pipeline-3D (proximal) and Hector-3D (distal) surveys. Additionally, the two seismic datasets were integrated three available wells: The Pukeko-1, Kiwa-1 and the Hector-1. Several seismic attributes which have been proven at imaging channels were generated to better constrain architectural elements along with interpreting the geometry of the channel complexes. Several intersecting 2-D lines were used to correlate interpretations between the two 3-D surveys to allow for accurate stratigraphic interpretations (Figure 1B).

## 2. Geologic Setting

### 2.1. Geologic Background

The Taranaki Basin is located off the western coast of New Zealand’s North Island and north of the South Island and consists of a sedimentary succession in thickness from

5 to 11 km [6]. The basin can be organized into three areas with different settings: The Western Stable Platform, Eastern Mobile, Belt, and Southern Inversion Zone. From the late Paleozoic until the mid-Cretaceous, New Zealand was characterized by convergent margin tectonics [13]. The Taranaki Basin began to form in response to the rifting of the Tasman Sea and breakup of Gondwanaland in three distinct phases: (i) extension, (ii) a brief period of approximately 3 million years of uplift and erosion, and (iii) extension that produced N to NE oriented normal faults [6,14]. Rifting ceased in the Paleocene [6,8,14], and the basin was a passive margin through the Eocene [6,14]. In the mid-Oligocene, the Pacific Plate began subducting beneath the Australian Plate and displacement along the Alpine Fault, east of the North Island. This marked a significant increase in subsidence rates in the Taranaki Basin [6,10]. This change in stress regime initiated the Southern and Central Taranaki Inversion Phase (SCTIP) approximately 8.5 Ma [15]. This led to the formation of the Southern Inversion Zone, which consists of extensional faults reactivated as compressional faults [6,8]. In the mid-Miocene, as uplift associated with the formation of the modern-day plate boundaries continued, a pronounced regressive shelf-to-slope system was established and progradation of the continental shelf began [6,15]. As uplift continued through the latest Miocene and early Pliocene, a regionally continuous unconformity was formed and is in the Te Whatu-2 well as a 3.2 Ma hiatus (Figure 2). During this time of progradation, a series of third-order cycles promoted the formation of deep-water channel systems [15,16]. These resulted in the deposition of the Moki Formation sandstones in the Late Altonian (Al) to Early Lillburnian (Sl) (16.7–15.1 Ma), the Waiauian (Sw) sands (13–11 Ma), the Mount Messenger Sequence during the Tongaporutuan (Tt) stage (11–7.2 Ma), and then the Matemateanga Sequence (Figure 2A). The provenance of the Mount Messenger Formation has been shown to correspond to multiple sources of recycled and eroded basement sediments [11]. Outcrop and subsurface studies throughout the Taranaki Basin on the Mount Messenger Formation have described it as being from a fine- to very-fine-grained sandstone to siltstone with interbedded claystone, which ranges in 300–800 m in thickness [6]. Sediment eroded from of uplifted sectors in the South Island was transported basinward in southeast-northwest oriented channel systems originating from a NW-SE oriented shelf, approximately 80 km southwest of the study area. By the Pliocene, high sedimentation rates induced by the emplacement of the modern-day tectonic boundary to the east led to the progradation of the shelf through the study area [17]. Large-scale progradation of the continental shelf continued through the Plio-Pleistocene. This resulted in the deposition of the stratigraphic unit informally known as the Giant Foresets Formation (GFF) occurred. The GFF is characterized by large, continuous clinofolds easily identifiable in seismic data. Correlative units found on land include the Tangahoe Mudstone, Whenuakura Subgroup, Nukumaruan and Castlecliffian strata. The GFF is underlain by the Urenui-equivalent slope mudstones, Manganui, Mangaa or Ariki formations [16].

## 2.2. Mount Messenger Depositional System

Detailed analysis of seismic scale outcrops along the western coast of the North Island and petroleum exploration has led to a wealth of research over the late Miocene Mount Messenger depositional system ([1–4,6,11,18–20], among others). Deposition of the Mount Messenger Formation can be summarized by two stratigraphic units. The Lower Mount Messenger Formation is generally composed of thick-bedded sheet-like sandstones and siltstones and channel occurrence increases up-section [18]. The Upper Mount Messenger Formation is described as consisting of thick to thin-bedded sandstone and siltstone turbidite deposits. Outcrop-to-seismic analysis done resulted in a depositional model which describes the Pukeruhe Beach section as a series of vertically stacked (aggradational to weakly progradational) depositional elements near the base of the slope [1]. Complex interfingering of lithologic elements resulted in shingled slope fan depositional elements [1]. Correlation of seismic-scale (up to 330 m thick and exposed for several km) mass transport deposit outcrop deposits within the Mount Messenger and Urenui Formations and are correlated to nearby 2-D and 3-D seismic surveys [3]. Other studies utilizing a process

sedimentology approach to classify the upper Mount Messenger Formation and concluded it is limited to a lower-slope depositional environmental environment at the exposed outcrop location [20]. The local slope was determined to have been steep enough to promote sediment bypass basinward and induce incision into the slope. The wealth of knowledge gained from excellent outcrop exposures along the Taranaki Peninsula has allowed for a great understanding of the depositional system, however the southern equivalents are still poorly understood.

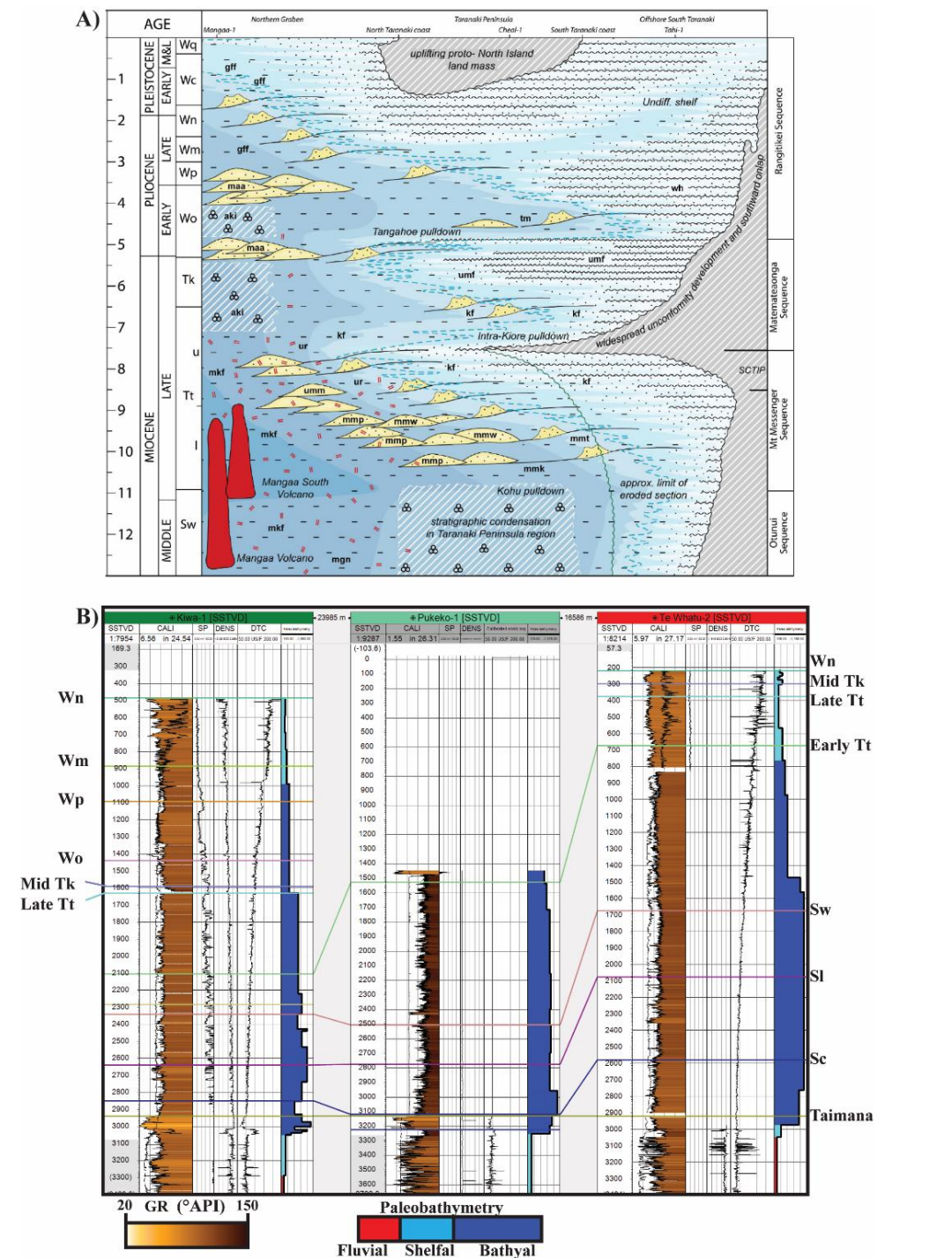


**Figure 2.** (A): Stratigraphic column of the southern Taranaki Basin modified after [15]. (B): Stratigraphic cross section flattened on the Taimana formation along depositional dip through the Te Whatu-2, Pukeko-1, and Kiwa-1 wells.

### 3. Data and Methods

#### 3.1. Seismic Datasets

Two three-dimensional (3D) seismic datasets were used to create a depositional model for mid-to late-Miocene channel complexes within the southern equivalents of the Mount Messenger Formation. The Pipeline-3D dataset is located north of the South Island, and southwest of Mt. Taranaki in the North Island (Figure 1). The area of the Pipeline-3D dataset is approximately 515 km<sup>2</sup>. The survey was acquired in 2013 by Todd Exploration and processed by Excel Geophysics in 2015. This dataset has SEG negative polarity, therefore an increase in acoustic impedance is represented by a trough. Kirchhoff anisotropy pre-stack time migration was applied during processing, and the data were processed to have a zero-phase wavelet. The data has a 4-millisecond sample rate and a record length of 6 s. The second, more distal 3-D survey analyzed was the Hector-3D seismic survey and is located northeast of the Pipeline-3D survey (Figure 1A). This survey was acquired in 2005 to image a local structural trap for hydrocarbon exploration in the southern Taranaki Basin within the Kapuni Formation. The marine survey was acquired with an eight-streamer survey device using two alternating sources. The full fold area of the survey is 434 km<sup>2</sup> and has a bin size of 6.25 m × 25 m. Like the Pipeline-3D dataset, Hector-3D has a 4-millisecond sample interval, 6 s record length, SEG negative polarity and was processed using a zero-phase wavelet. Since the two datasets have similar acquisition and processing records, this allows a better correlation of the two datasets.

Several available two dimensional (2D) seismic lines were used to correlate interpreted horizons of the Pipeline-3D to the Hector-3D survey. These include the MOHOa-DSIR Line, and lines 19 and 21 from the T96 survey, along with Lines 2307 and 2308 from the S18 survey. Both 2D surveys have a 4-millisecond sample rate, a 6-s record length, and are of SEG positive polarity, where an increase in acoustic impedance is represented by a peak in the seismic data. To match polarities between the 2D and 3D surveys, the 2D lines were phase-shifted 180 degrees so that an increase in acoustic impedance is represented by a trough in the seismic data (Figure 1B).

#### 3.2. Well Data

In the Pipeline-3D survey area, data from the Pukeko-1 and Te Whatu-2 wells were incorporated into the interpretation. The Pukeko-1 well was drilled in 2004 to a total depth of 4190 m, approximately 23 m below the top of the granitic basement. This well has been plugged and abandoned, as no commercial quantities of hydrocarbon were discovered. Logging began at the base of our study interval, and paleobathymetry was incorporated from previous studies [21]. The Te Whatu-2 well was drilled in 1987 in the southern section of Pipeline-3D. GR, SP, DT, and paleobathymetry logs are present through the study interval. The late Pliocene unconformity is encountered in this well and represents a 3.2 Ma hiatus in deposition. Well cuttings indicate the interval of interest of this study is dominated by claystone with minor siltstone interbedded at the well locations.

The Hector-1 and Kiwa-1 wells are both within the distal Hector-3D seismic volume. The Hector-1 well was drilled in 2007 to a total depth of 3825 m, approximately 2 m below the top of the granitic basement. No logs were run within the late Miocene interval in the Hector-1 well, however cuttings within the study interval were described as claystone and siltstone with minor sandstone. The Kiwa-1 well was drilled in 1982 to a TD of 3858 m, 25 m below top of basement. The Kiwa-1 well was logged in the study interval with GR, SP, RHOB and sonic logs available (Figure 1). Revised biostratigraphy places the study interval from in the late Miocene (8.9–7.2 Ma) [21]. Side wall cores (SWC) taken from the interval 1530–1650 m MD display gradational bed boundaries (PR880). The GR log displays an overall coarsening-upward succession in GR, and the SP log is characterized by a serrated response (Figure 1). Fauna in this interval suggest a depositional environment near the shelf-slope break as sediment transport resulted in outer neritic and bathyal fauna species throughout this interval [22]. SWC's gathered in the interval of 1650–2095 m (MD) indicate massively bedded sandstone deposits, with thin siltstones interbedded, and have sharp

contacts (PR880). The GR log is characterized by minor fining and coarsening upward successions, and the sandstone bodies are indicated by cylindrical shapes in the SP log.

### 3.3. Seismic Analysis

Due to the limited well control in the studied interval in the Pipeline-3D survey, the Hector-3D survey was chosen as a starting point in the mapping workflow, following the well-to-seismic tie at the Kiwa-1 well. Seismic mapping consists of mapping, or “picking” an amplitude reflector throughout a survey. In this study, a fluid picking interval was used. In areas with little channel incision or interruption of the reflectors, picks were made on every 25 in- and crosslines. In regions with complex reflector geometry due to channel incision, picks were made every 5 in- and crosslines. These picks were then correlated via arbitrary lines. Once completed, autotracking was done and checked. In regions that did not track well, such as channel axes, the interpolation was erased and re-picked. Several continuous, high-amplitude reflectors corresponding to key chronostratigraphic intervals from the Kiwa-1 well were identified and mapped throughout the Hector-3D survey. These include the mid-Waipipian (Wp; 3.7 Ma), top Tongaporutuan (Tt; 7.2 Ma), the base of the Early Tt (11.04 Ma), and the top of the Lilburnian (Sl; 15.1 Ma) (Figures 2 and 3). After mapping the Hector-3D survey, 2D seismic lines were employed to correlate the interpretations into the Pipeline-3D survey.

To characterize the channel systems in this study from seismic data, the architectural elements will be analyzed following the classification scheme after Janocko et al. (2013) [23]. An architectural element is a depositional body defined by its facies composition, scale, depositional process and setting or geometry [24]. Janocko et al. (2013) [23] presents detailed analyses of the seismic characteristics of deep-water sinuous channel systems in offshore West Africa, utilizing outcrop analogs from around the world, including the Mount Messenger Formation. The methodology identifies five main architectural elements: lateral-accretion packages (LAPs), channel-bend mounds, levees, mass-transport deposits (MTDs), and last-stage channel-fills. Four classes of sinuous channel belts are proposed: meandering non-aggradational channels, leveed aggradational channels, erosional cut-and-fill channels, and hybrid channels. By interpreting reflector geometries and identifying architectural elements within a channel belt and analyzing their vertical stacking patterns, this methodology allows for inferences of the genetic relationship and evolution of the channel belts.

### 3.4. Proportional Slicing

Due to heavy channel incision and the discontinuous reflectors within the Tt interval (11.04–7.2 Ma) combined with dipping reflectors, proportional slicing was performed on both data sets to visualize the channel systems’ temporal evolution in the study interval. The base of the Tt will be referred to as “Lower Tt” and the top of the Tt will be referred to as “Upper Tt”. Proportional slicing is an effective technique to visualize data in plan-view when coherent reflectors are not present or when dealing with inclined reflectors [25]. Given the spacing between Lower Tt and Upper Tt, nine proportionally spaced surfaces were generated between these two horizons representing a surface increment of ten percent between the two mapped horizons (Figure 4). Calculated proportional slices are numbered one through nine, with nine being the deepest. The proportional slices, referred here as stratal slices, were calculated using the trivial equation:  $SS_x = (1 - x) * Upper_{Tt} + (0.x) * Lower_{Tt}$ . For example, SS9 represents 90% of Lower Tt and 10% of Upper Tt. Calculated volume attributes and spectral decomposition blends were then extracted along these surfaces to enhance geomorphologic and stratigraphic interpretations.

### 3.5. Seismic Attributes

A selected suite of 3-D seismic attributes was generated based on their ability to aid in channel architecture identification. The attributes were calculated and then extracted along

interpreted horizons to help identify internal structures of the channel complexes that are not easily visible in the original amplitude data. Coherency-based attributes, which include energy ratio similarity, Sobel filter, and coherent energy highlight subtle discontinuities in the seismic data [26]. For this study, energy ratio similarity (ERS) was selected, as it has been shown to be superior to other algorithms in visualizing discontinuities [27]. Additionally, most-positive ( $k_1$ ) and most-negative ( $k_2$ ) curvature attributes were generated. Curvature measures the concavity of a surface. Positive values in most-positive curvature represent concave down features such as channel banks and/or levees. Negative most-negative curvature anomalies represent concave up features, like the base of a channel—which is not easily seen in amplitude data [28] (Figure 5). In both  $k_1$  and  $k_2$ , planar features are represented by a value of zero, whether they are inclined or flat.

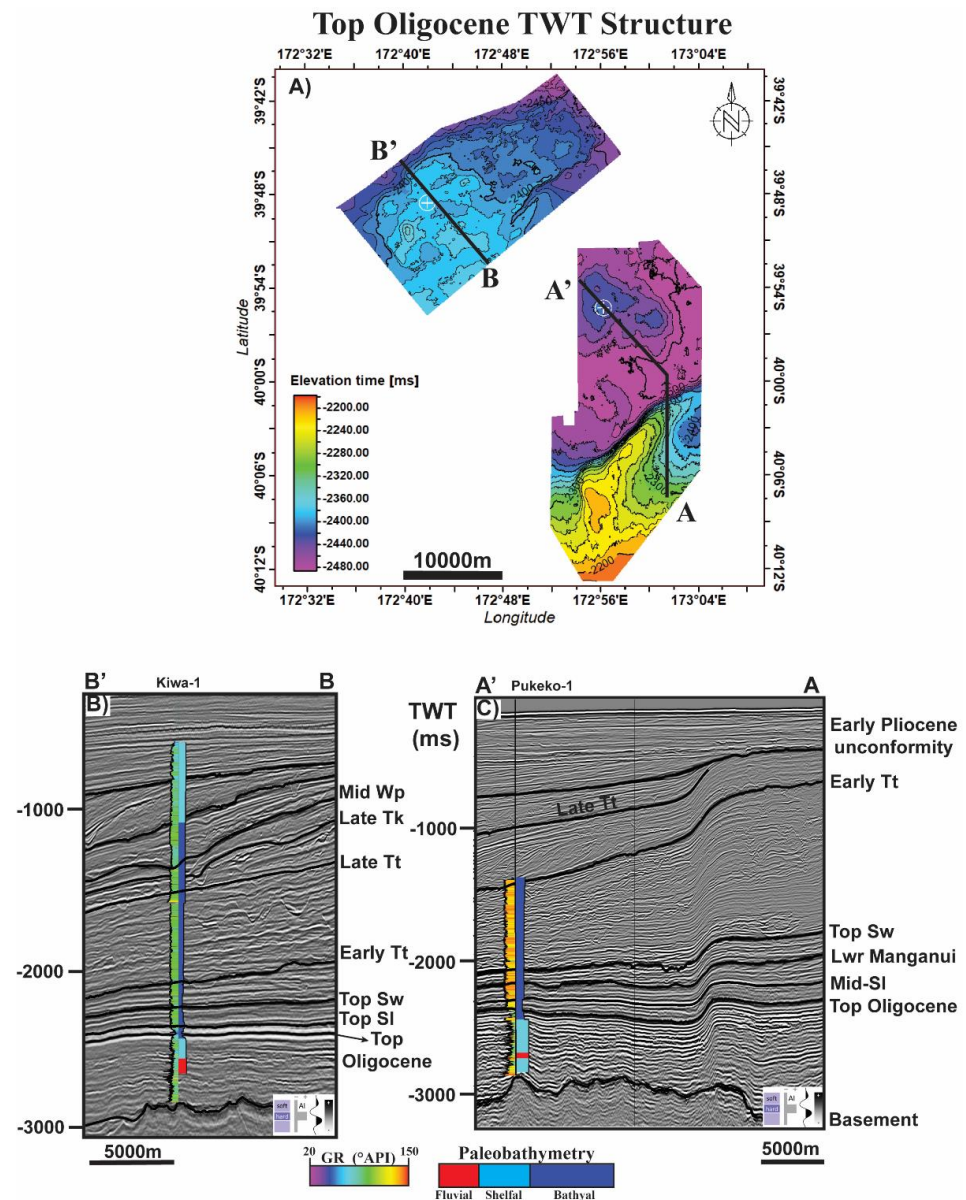


**Figure 3.** (A): Top Oligocene TWT structure map of the Pipeline-3D and Hector-3D seismic surveys. (B): Arbitrary line along depositional dip through the Hector 3-D seismic survey with interpreted horizons shown. The Hector-1 well is shown with measured gamma ray log and paleobathymetry log. (C): Arbitrary line through the Pipeline-3D seismic survey with interpreted horizons shown. The Pukeko-1 well is shown with measured gamma ray log and paleobathymetry log.

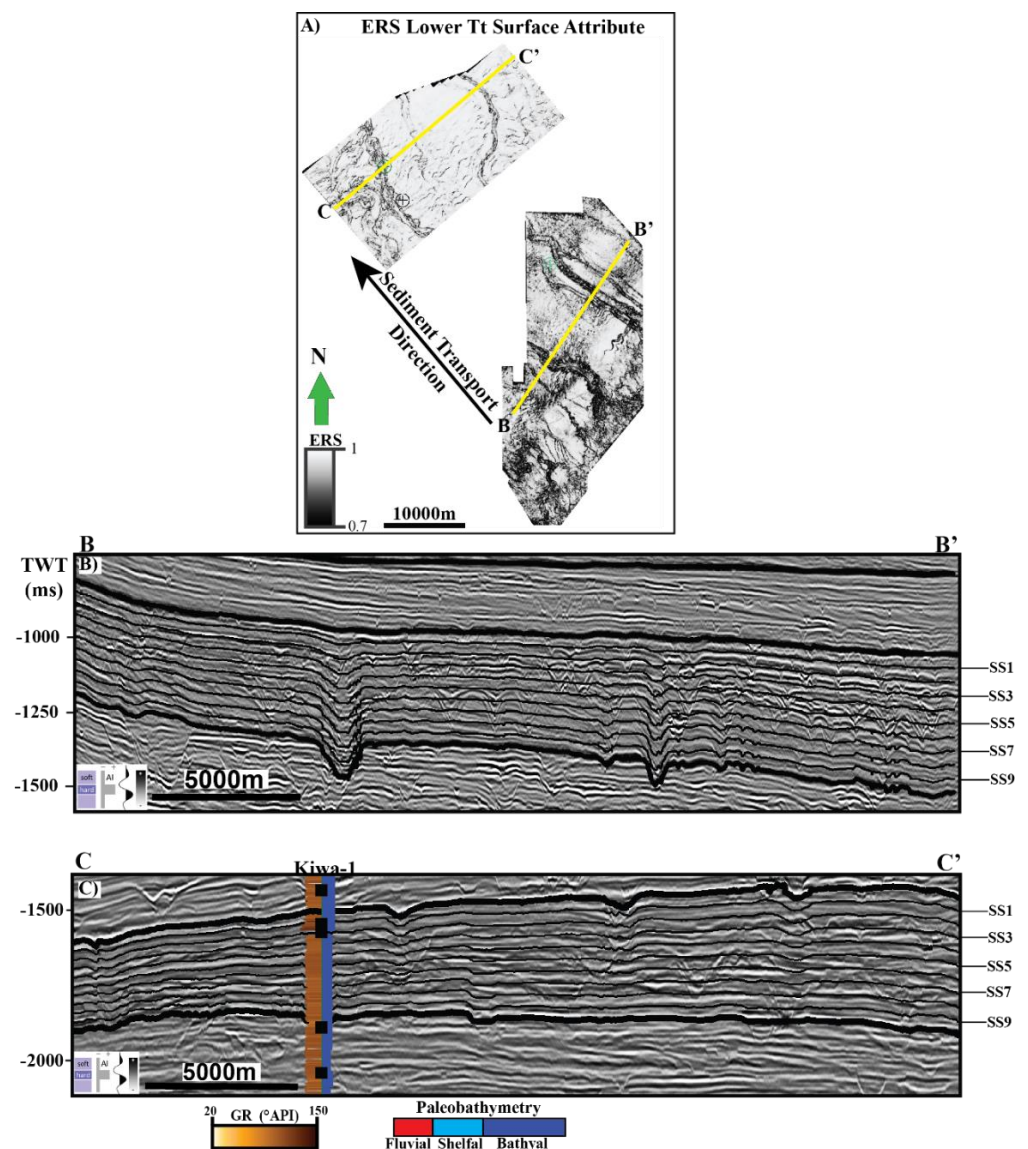


**Figure 4.** (A): Map view of the lower Tongaporutuan (Tt) surfaces with the energy ratio similarity (ERS) attribute extracted along them. (B): Seismic section perpendicular to sediment transport direction in the Pipeline-3D survey displaying the resulting stratal slices. (C): Seismic section perpendicular to sediment transport direction in the Hector-3D survey displaying the resulting stratal slices.

Spectral decomposition was performed on both datasets to analyze the channels in the frequency domain. Spectral decomposition enhances the visualization of channel systems, as it decomposes the amplitude data into its spectral components [29]. This is accomplished by using the Fourier transform, and results in individual frequency cubes. Once generated, the individual cubes were scanned-through, visually, to determine the frequencies which best visualize the channel systems. Frequency cubes at 15 Hz, 35 Hz, and 65 Hz were chosen for blending and, subsequently, extracted along the generated surfaces. These cubes are then blended together using a red–green–blue (RGB) color scheme, where the colors represent the low, middle, and high frequencies respectively. In RGB blending, a bright white response indicates that the energies of all three frequencies are at or above tuning. A bright response of a single color occurs when a single component’s energy is stronger than the other two, and a dim response when none of the blended frequencies have dominant energies. Previous work has demonstrated the application of spectral decomposition to assist in stratigraphic interpretation [30,31]. The general relationship

is that lower frequencies represent thicker intervals while higher frequencies represent thinner intervals of a channel [30]. This attribute was used to validate interpretations made on amplitude-based attributes, as well as enhancing stratigraphic interpretations.

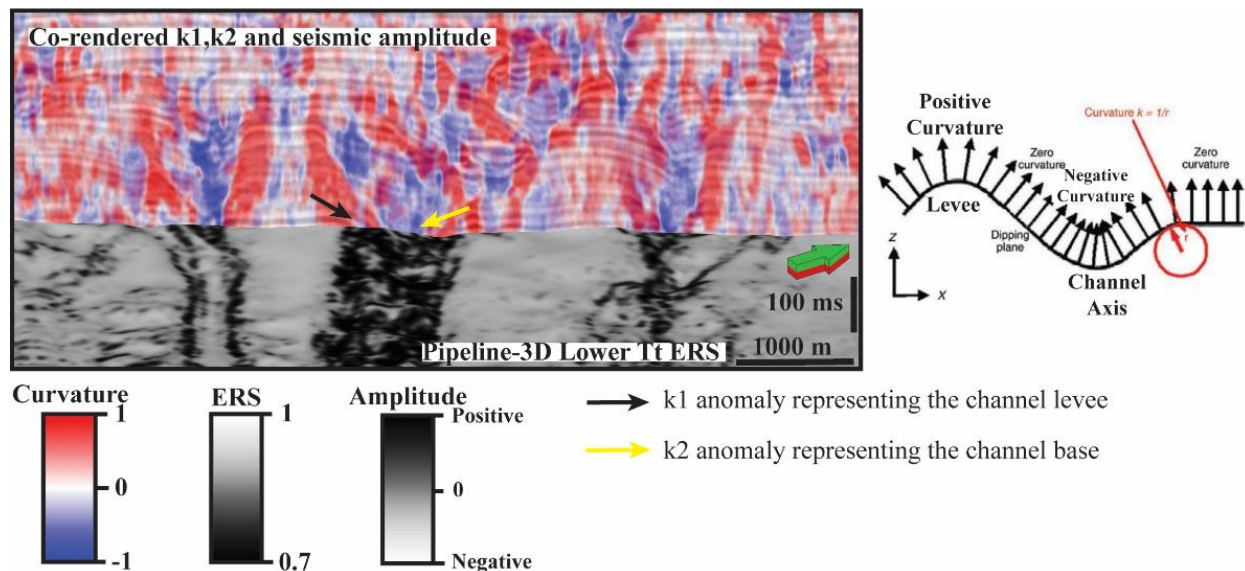


**Figure 5.** Co-rendered curvature (most positive and most negative) with seismic amplitude inline, displayed with the ERS attribute extracted along Lower Tt. The curvature attributes highlight concave-down (k1) and concave-up (k2) reflectors, while the ERS attribute highlights discontinuities caused by dipping planes.

## 4. Results

### 4.1. Pipeline 3D Study Area

Nine proportionally spaced surfaces were generated within the Tt interval of the proximal Pipeline-3D survey (Figure 6). The ERS, curvature, and spectral decomposition blends were then extracted along Lower Tt and B (Figure 4). In the deepest horizon mapped, Lower Tt, a deep-water channel–levee system is visualized (Figure 6A). The valley margins are straight, deeply incised, and exhibit well-developed master levees. Channels range from 250 to 1250 m wide and are approximately 230 ms TWT (approximately 265 m) deep (Figure 7).

The channel-fill is typically low-amplitude and consists of vertically-stacked-to-shingled reflectors (Figure 7). Three channel complexes (CC1–CC3) are examined in the Pipeline-3D survey. CC1 and CC3 are truncated by CC2 in the East (landward) and relationships of the reflectors between the channel complexes suggest CC1 and CC3 were active prior to CC2. The initial erosional surface of all three complexes is a U-shape with minor levee development. A second erosional surface is present within CC2 and has a distinct V shape with vertical aggrading reflectors. Erosion depth decreases downslope in all three complexes along Lower Tt, and channel fill becomes more variable with higher amplitude values present further downslope. Extracting ERS and curvature along the horizon clearly images the master valley margins, in addition to revealing curvilinear anomalies interpreted to be sediment waves between channel complexes (Figure 6A,B). Two sinuous channels, oriented north–south, are present on the eastern portion of the mapped area. These channels terminate against CC2. These are unique, as they are oriented perpendicular to the main sediment transport direction, and likely served as slope feeder channels. Outcrop-scale feeder channels have been documented on the west coast of the North Island within the Mount Messenger Formation [2]. In the south, a highly sinuous channel system is indicated by the scalloped meander loops visualized in each of the surface attributes (Figure 6A–C).

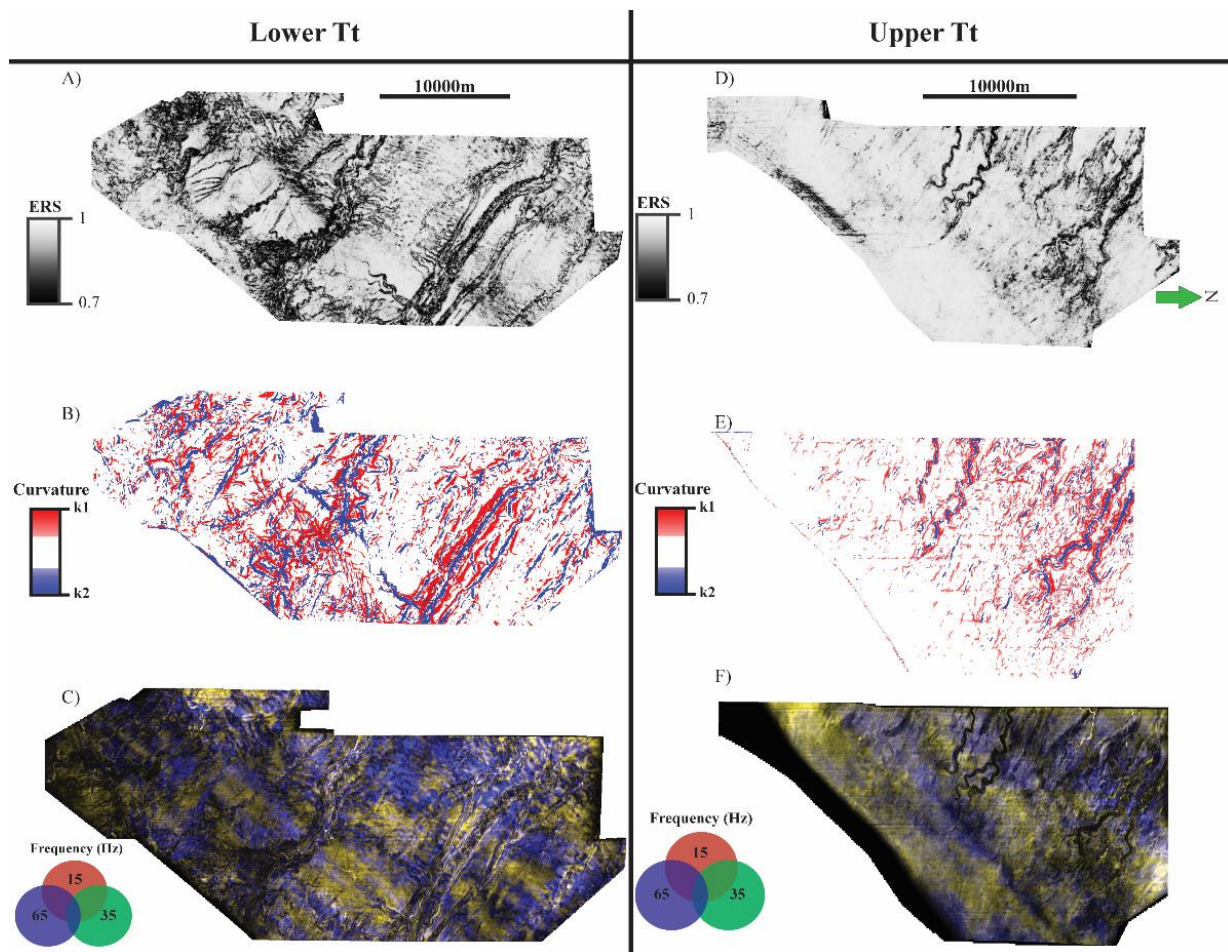


**Figure 6.** Attribute extractions along Lower Tt (lower Tt) and Upper Tt (late Tt) in the Pipeline-3D seismic survey. (A): Energy ratio similarity (ERS). (B): k1 and k2 curvature. (C): Red–green–blue (RGB) blend of spectral decomposition frequency volumes. (D): ERS along Upper Tt. Note how channels are no longer continuous across the survey and initiate in the central portion. (E): k1 and k2 curvature. (F): RGB blend of spectral decomposition frequency volumes.

The RGB spectral decomposition blend highlights a series of amalgamated channels within the margins along with multiple smaller channel axes in the south east portion of the survey (Figure 6C). In the north, several narrow, straight leveed channels are observed. (Figure 6B). The spectral decomposition extraction also images the sediment waves observed in the ERS attribute as curvilinear lineaments alternating in blue (high frequency) and yellow (mid-low frequencies). Co-rendering the k1 and k2 attributes clearly reveals the levees and bases of the channel complexes (Figure 6B). Furthermore, the k2 attribute in the southeastern edge of the horizon further highlights the base of the sinuous feeder channel than what is observed in the ERS surface extraction. Channel fill displays a stronger spectral-response downslope (NW) and is characterized by a bright response from the 65 Hz component, suggesting relatively thinner deposits (Figure 6C).

Upper Tt illustrates a distinct change in depositional elements compared with Lower Tt. Extracting the ERS attribute upon the horizon reveals eight highly sinuous channels (Figure 6D). These channels are approximately 150 to 200 m wide and have incision depths of 25 ms TWT (approximately 29 m or 95 ft) (Figure 8A,B) which is significantly less than those observed in Lower Tt.

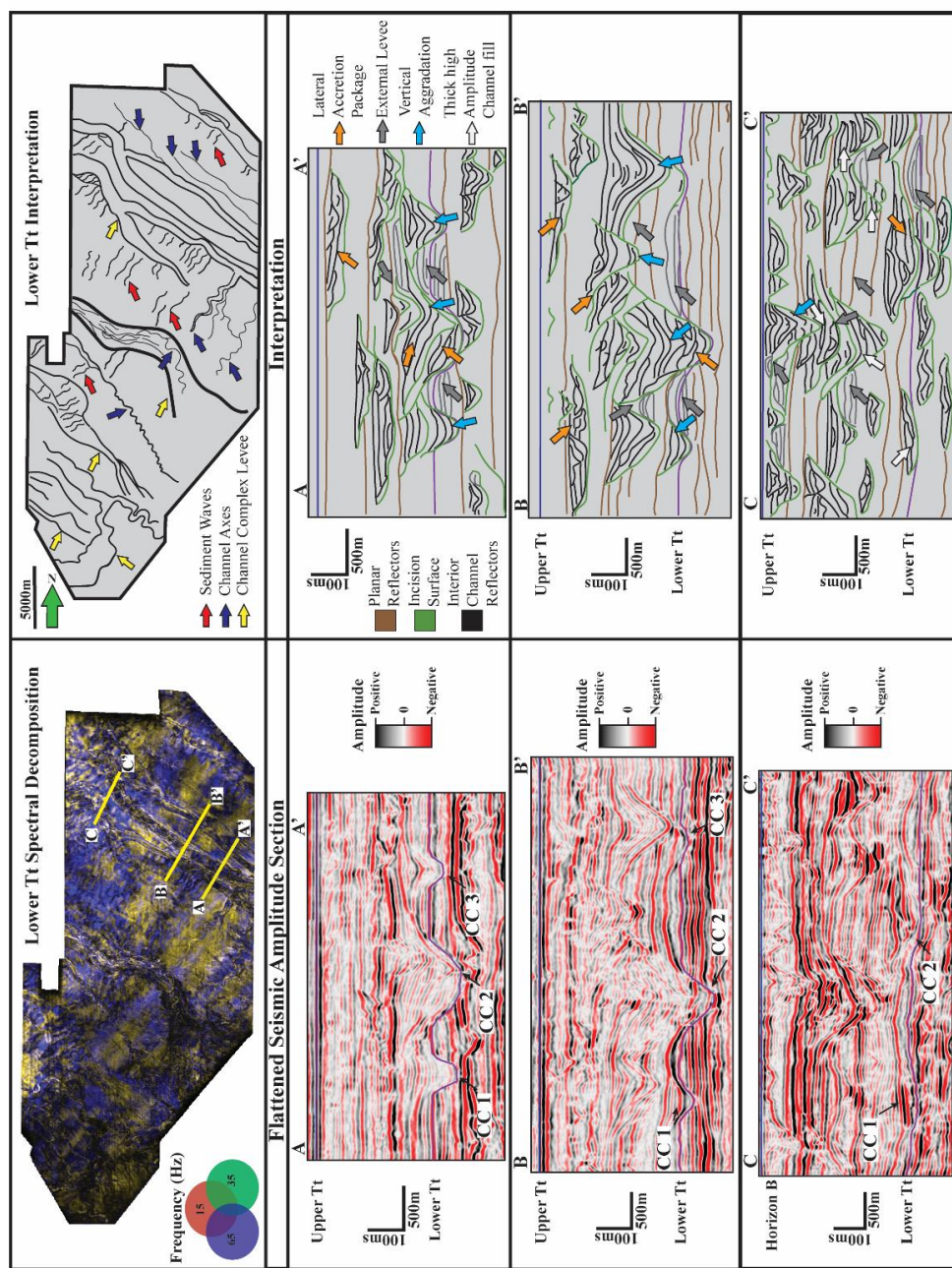
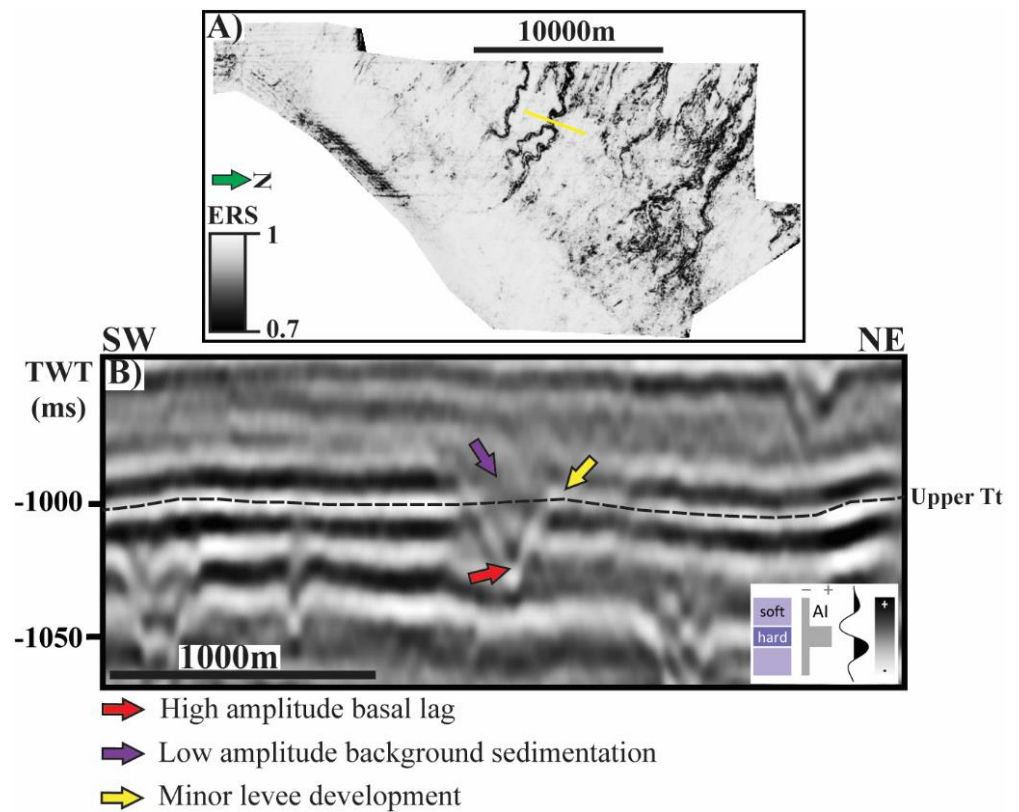


Figure 7. Table of seismic sections progressing down slope illustrating the spatial and temporal changes of the channel complexes.

Additionally, these channels do not span across the entire study area—they initiate near the central part of the Pipeline survey and progress through the northwest edge of the survey area (Figure 6D). These channels have minor levee development, and evolve from sinuous to linear channel systems (Figure 6D). The ERS surface attribute shows higher similarity values surrounding the channels compared to Upper Tt, indicating a more coherent and un-deformed surface in the intra-channel region (Figure 6D). The k1 and k2 attributes correlate strongly with the observed channels, clearly imaging the levees and erosional bases of the channels (Figure 6E). When viewed in cross section, spectral decomposition further visualizes the initiation of the turbidite channels on Upper Tt (Figure 6F). Acquisition footprint is present as faint N–S lineaments. Channel fill is characterized by a dim, bland response in spectral decomposition.



**Figure 8.** (A): ERS attribute extracted along Upper Tt in the Pipeline-3D survey. (B): Seismic amplitude section at the location noted by the yellow line in (A). Note the shallow incision depth, V-shaped channel complex, and minimal levee formation.

#### 4.2. Hector 3D Study Area

As in Pipeline-3D, nine stratal slices were made between Lower Tt and B in the Hector-3D study area (Figure 4). In the more distal Hector-3D dataset, the master valleys in Lower Tt are slightly more sinuous than those observed in the Pipeline-3D area. Extracting the ERS attribute upon Lower Tt highlights the margins of the northwest trending channel systems (Figure 9A).

The channels are incised 150 ms TWT (approximately 170 m) and levee development is not as prominent as in the Pipeline-3D area. Lateral migration of channel complexes is common, and typically trend to the NE (Figure 10). Channel fill is characterized by planar low-amplitude reflectors that terminate against the channel flanks or are truncated during later incision events (Figure 11). In the southwestern area of the survey, the k2 attribute shows an 1800 m wide sinuous channel complex, cross-cut by a younger 400 m-wide channel (Figure 9B). Collapse of the southwestern channel bank is also observed in the spectral domain, and the channel fill is characterized by a dim response of the 35 Hz spectral component. Abandoned meander belts are visualized by each attribute in the nearby channel to the northeast (Figure 9A,B). Arcuate-to-linear ERS anomalies are pervasive between the channel systems and are interpreted to be inter-channel sediment waves deposited by unconfined sediment flows [32]. A pair of linear gullies are present in the northeastern edge of the survey and well-visualized by the curvature attribute (Figure 9A). Spectral decomposition highlights two bright 3 km-long anomalies protruding from a meander loop (Figure 9c). When viewed in cross-section, these correspond to a planar High Amplitude Reflection Package (HARP) and are interpreted to be overbank splays (Figure 10A,B). The channels to the northwest exhibit alternating bright responses from the 35 and 65 Hz frequencies respectively.

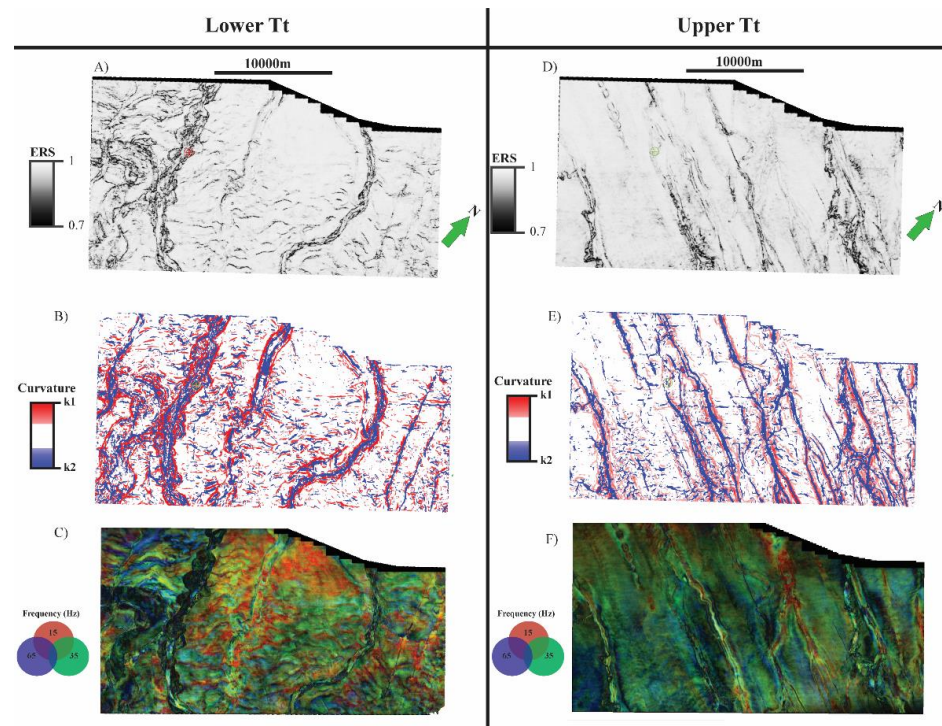


**Figure 9.** Attribute extractions along Lower Tt (lower Tt) and Upper Tt (late Tt) in the Hector-3D seismic survey. (A) Energy ratio similarity (ERS). (B) k1 and k2 curvature. (C) Red–green–blue (RGB) blend of spectral decomposition frequency volumes. (D) ERS along Upper Tt. (E) k1 and k2 curvature. (F) Red–green–blue (RGB) blend of spectral decomposition frequency volumes.

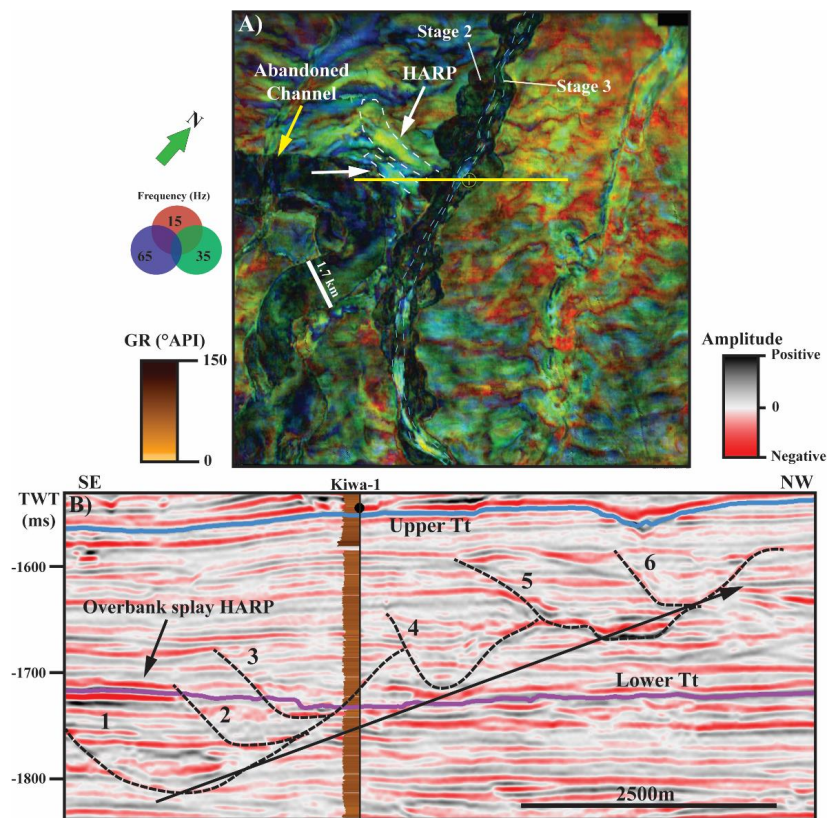


**Figure 10.** (A) Spectral decomposition RGB blend in the Hector-3D extracted along Lower Tt zoomed into the Kiwa-1 Well. (B) Seismic amplitude section displaying six stages of channel complex migration.

Migration at this location was consistently to the north-east. Depositional elements present include overbank high-amplitude reflection packages (HARP), multi-storied channel complexes, and overbank sediment waves.

Upper Tt in the Hector survey displays slightly narrower channels and some appear gully-like (Figure 9D,E). Sediment waves are significantly less common as inter-channel regions show high ERS values. In the western edge, a discontinuous scalloped feature is present and interpreted to be an erosional channel feature [33]. When viewed in vertical section, the scalloped feature exhibits an undulating reflection pattern, along with onlapping reflectors. Below, weak amplitude shingled reflectors are present and likely represent sediment waves (Figure 12B). Above, planar high-amplitude reflectors onlap onto the undulating reflector. Similar erosional scours have been observed in other deep-water depositional systems around the world, including the East Breaks Basin Four, offshore Gulf of Mexico [34], Albania, and, in Canada, within the Cretaceous Iron fluvial reservoir [34]. Spectral decomposition reveals narrower dendritic feeder channels which combine into the larger channel complex visualized by the ERS surface attribute (Figure 9F).

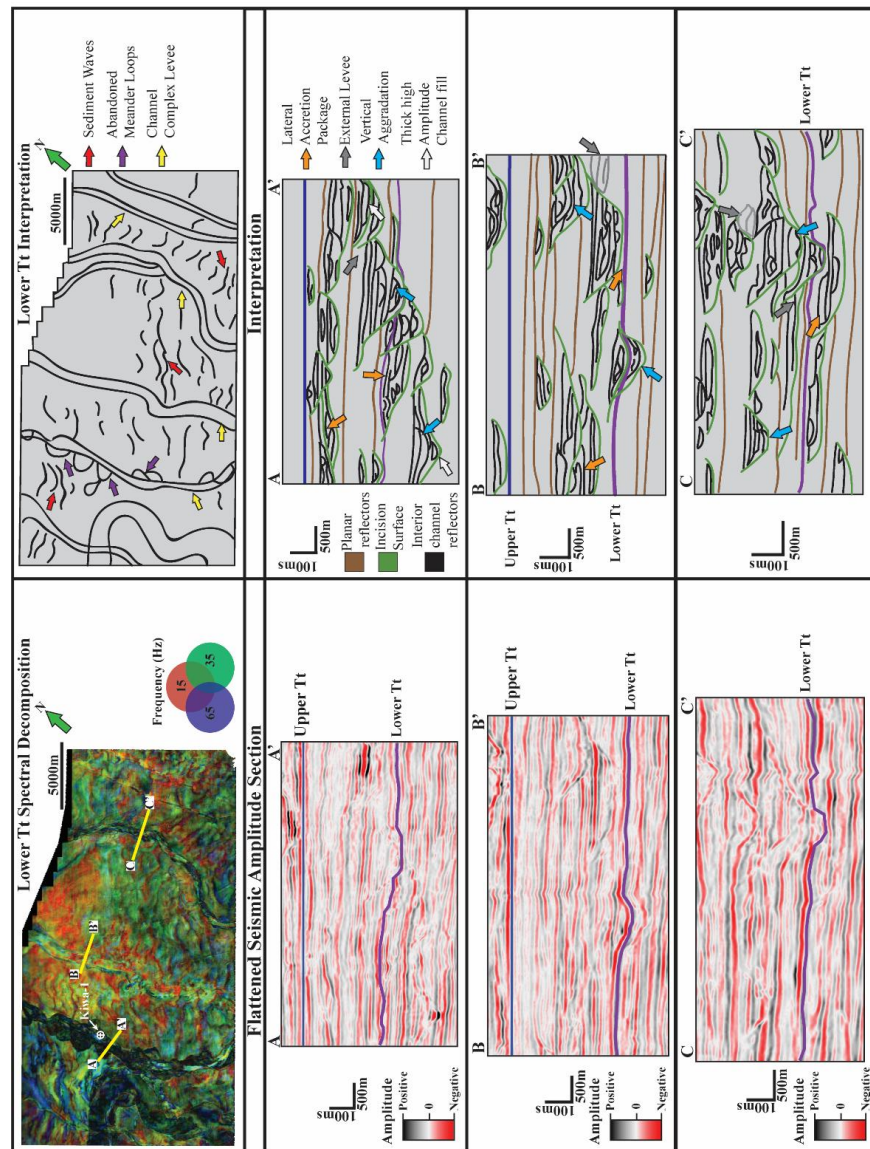
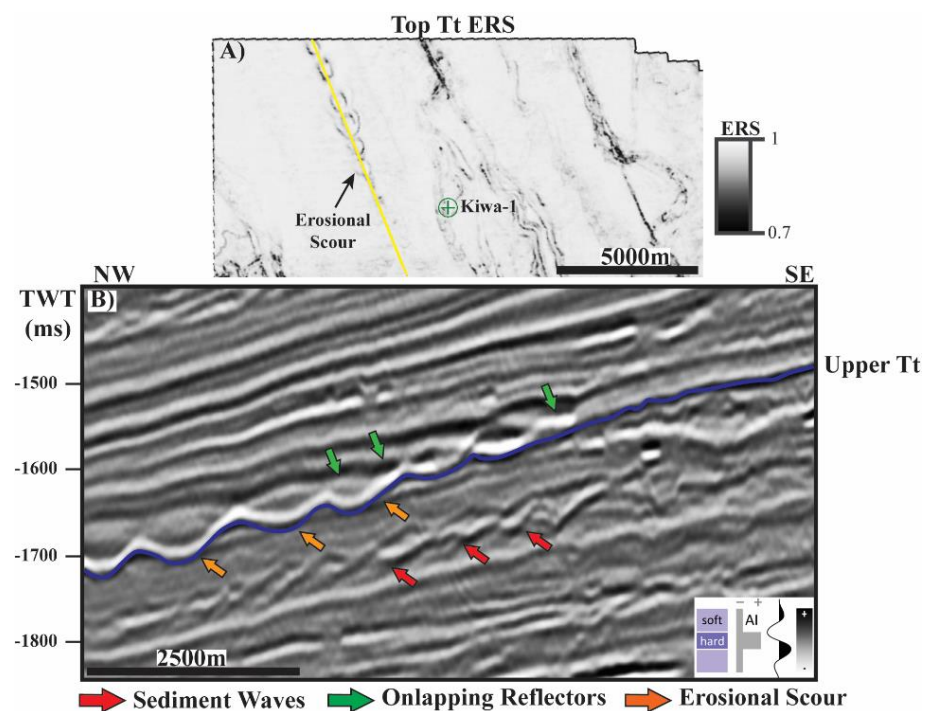


Figure 11. Table of seismic sections with interpretations illustrating the spatial and temporal changes of the channel complexes in the Hector-3D survey.



**Figure 12.** (A): Inset of the Top Tt surface draped with the ERS attribute displaying the erosional scours. The yellow line shows the location of B. (B): Arbitrary seismic amplitude section showing the undulating, scalloped erosional channel scour. Adjacent planar reflectors are truncated against the anomaly.

## 5. Discussion

### 5.1. Temporal Evolution

Both the Pipeline-3D and Hector-3D datasets provide a detailed record of the evolution of these deep-water channel systems. The correlation of the two allows for a detailed understanding of how the late-Miocene Southern Taranaki depositional system evolved through time in response to the Southern Taranaki Inversion Phase (SCTIP). In the more proximal Pipeline-3D survey, a complex deep-water depositional system is visualized (Figure 13).

When viewed in cross-section, multiple episodes of erosion, fill, and minor channel migration is evident on Lower Tt in cross section A-A' (Figure 7). Channel Complex 1 (CC1) and CC3 have weak, low amplitude planar infill reflectors. These channel complexes were likely eroded and promoted sediment bypass while active, and filled in with sediment as flow diminished. CC2 is a multi-story channel complex, has low-amplitude-onlapping-to-truncated reflectors, and displays signs of several incision events (Figure 7). The onlapping and truncated reflectors are interpreted to be lateral accretion packages (LAPs) [35]. The channel complexes on Lower Tt display characteristics typical of erosional channel belts [23]. Younger channels at this location exhibit minimal incision with broad U-shaped incision surfaces and were likely immature meandering channel complexes. As the system progresses, a decrease in incision depth is observed in CC1 and CC3 with well-developed external levees. CC2 has shingled high amplitude basal reflectors, suggesting coarse-grained channel lag deposits. Younger overlying channel complexes observed in section B-B' show increased incision depth with low amplitude chaotic infill (Figure 7). At the limit of the survey in section C-C', CC1 and CC2 are characterized by thick high amplitude reflector infill with poorly defined channel flanks (Figure 7). These channel complexes are shifting from an erosional-confined system to a levee-channel system. CC3 is no longer present, and the spectral decomposition-surface attribute suggests it transitioned to a frontal splay (Figure 7). Overlying channels are now characterized by thick, high-amplitude infill, and have established external levees. This transition is observed via the ERS attribute, as several linear channel systems appear in

SS9 through SS7 (Figure 13). The ERS attribute on SS6 through SS4 exhibits a chaotic seismic facies, with numerous straight-to-slightly sinuous channels present throughout the survey, indicating inconsistent sediment transport and slope instability. In SS3 through SS1, dendritic channels, characterized by low ERS values for their fill, converge to form master valleys, becoming more organized and coherent through time. Upper Tt displays waning stages of sediment transport during the Late-Miocene interval within the Pipeline-3D area, in which the channels initiate in the central portion of the survey amid a coherent surface (Figure 8). These weakly-incised, V-shaped channels exhibit minor levee development, with high-amplitude basal lag with low-amplitude bland channel infill.

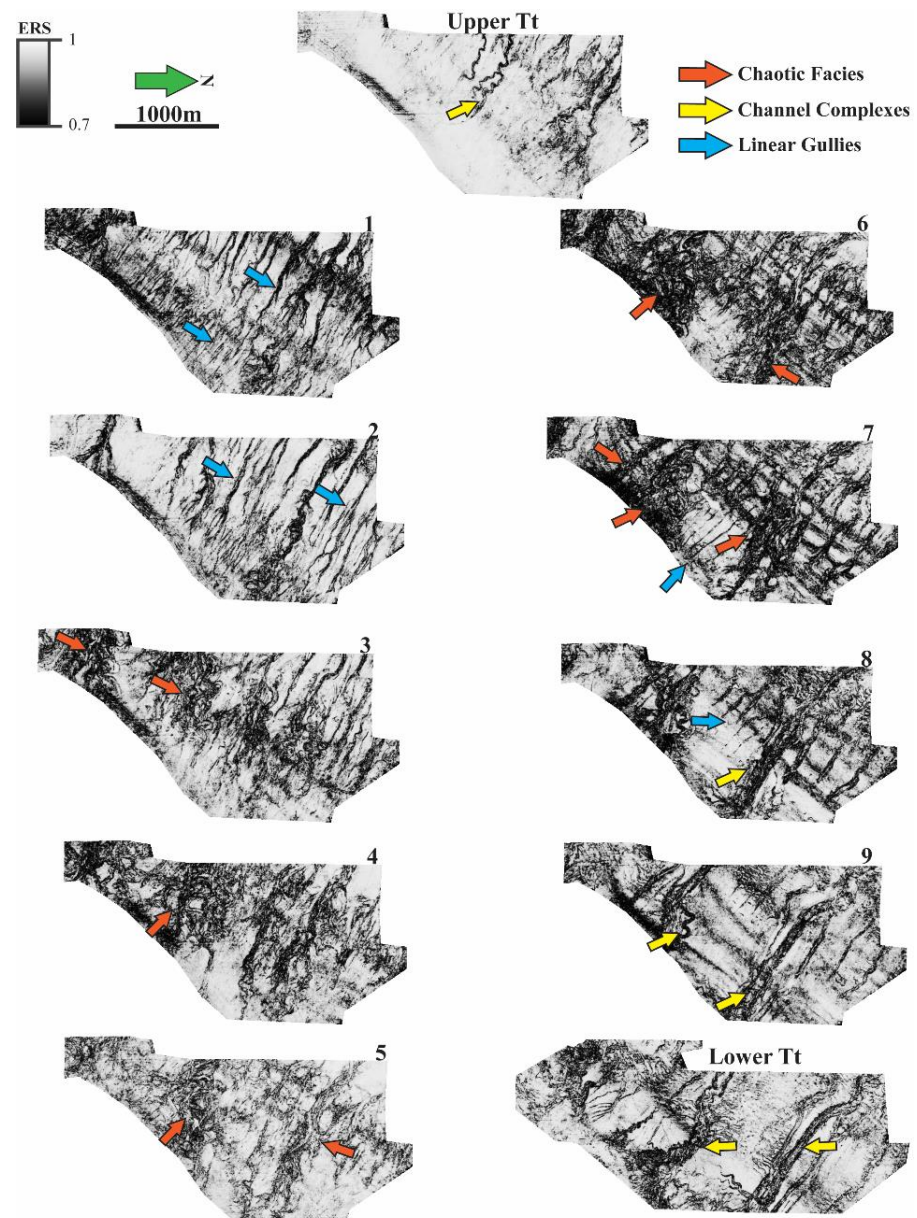


**Figure 13.** Pipeline-3D stratal slices draped with the ERS attribute. Channel complexes are typically characterized by low-sinuosity and minimal lateral migration. See Figure 4B for stratal slice location in cross section.

In the more distal Hector-3D dataset, a coherent evolution is observed through time (Figure 14). Initially on Lower Tt, five channel complexes are present (Figure 14). When viewed in cross section along A-A', the channel complexes have broad U shaped incision surfaces with slightly inclined planar channel fill (Figure 11). Multiple episodes of cut-and-

fill of channels indicate the presence of meandering channel belts in the three channels examined (Figure 11). As time progresses, SS8 through SS3 document the spatial migration of the meandering channel systems, channel abandonment, and the cross-cutting of the older channels (Figure 14). Overlaying traces of the channel axes from the stratal slices, the southern channel complex displays prominent meander loop expansion, or swing, and minor downslope migration, or sweep [36] (Figure 14). The eastern two channel complexes, while meandering, display minor swing and sweep, suggesting these systems abandoned the prior channel complex upon avulsion. Sediment waves dominate the inter channel regions on SS9 through SS6, and then again in SS3 and SS2. In SS1 and Upper Tt, the once prominent wide and sinuous channels are replaced with narrow gully systems.

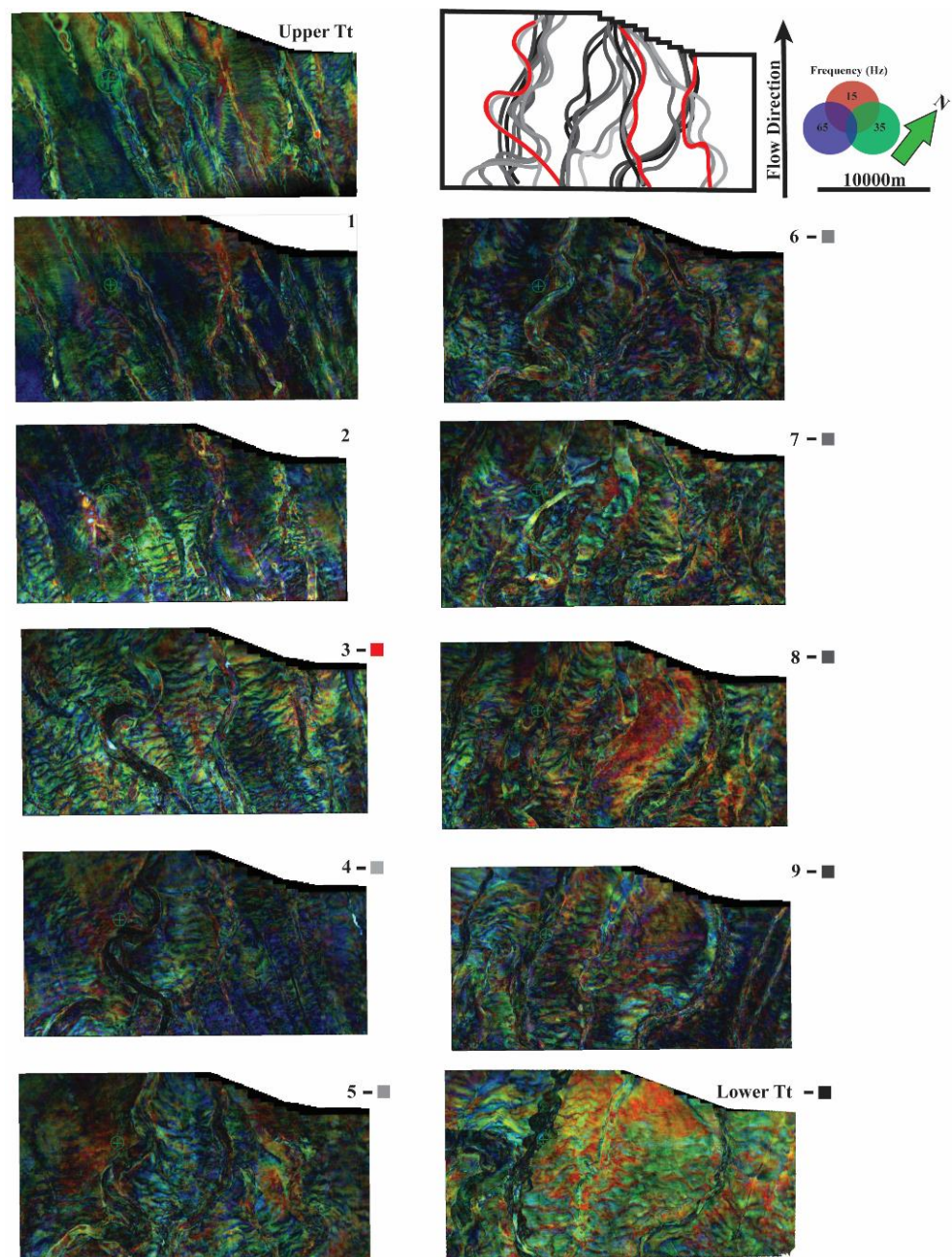


**Figure 14.** Stratal slices draped with RGB spectral-decomposition blends in the Hector-3D survey. The axes of the channel complexes in Lower Tt through SS 3 are traced and presented in the top-right to illustrate the migration of channel complexes through time.

## 5.2. Depositional Environments

Mapping of the proximal Pipeline-3D-area features' channel complexes, with vertical aggradation, shows well developed levees and low-sinuosity in Lower Tt (Figure 7). Paleobathymetric data from the Pukeko-1 well indicate that water depths were bathyal at this time and likely at or near the base of the slope (Figure 2B). These channel complexes were formed in response to crustal shortening associated within the Maari anticline and Southern Cape Egmont Fault to the east [37] (Figure 1A). This uplift continued during the Tt and possibly into the early Tk. Partial exhumation of the Southern Inversion Zone also occurred during this time period, further providing sediment input to be transported basinward [8,15,38]. This is reflected in the study area; as multiple closely-spaced channel systems are visualized. The internal reflector geometry of the channel complexes, combined with the observed levee and minor overbank deposits, suggest these were slope-confined systems in the Pipeline-3D area. As no major fan deposits were observed within the Pipeline-3D area, the channel systems within the late-Miocene study interval likely served as conduits which transported sediments basinward through the Hector-3D study area. The sediments transported through these systems in the late Tt and early Tk were typically fine-grained, which is consistent with the lengths and geometry of the complexes present in the two areas. During development of the channel systems in Lower Tt, minor flow-stripping likely removed the head of the turbidity current, promoting deposition of finer-grained sediments overbank and within the levees, as seen along CC2 (Figure 7) [39]. Planar reflectors within the channel fill suggest periods of background sedimentation between periods of sediment transport (Figure 7). Progradation of the shelf-slope resulted in younger channel complexes in Pipeline-3D and increased incision depth downslope (Figure 7). On Upper Tt, overbank deposition has significantly decreased in the survey area, as indicated by the relatively coherent ERS attribute. Several narrow, sinuous channels began to form in the central part of the survey. This is a distinct change in depositional environment relative to Lower Tt, as Upper Tt reflects a sediment staging area upon the shelf with a lower gradient than the environment observed in Lower Tt. This decrease in observed depositional gradient is estimated to occur approximately 7–8 Ma (lower Tk), which is consistent with a period-stable crustal shortening rate in the Southern Taranaki Basin [8] and progradation of the shelf-slope across the study area [15].

The distal Hector-3D Lower Tt displays sinuous channel complexes approximately 400 m wide with less incision than observed in Pipeline-3D. In addition, frequent migration and avulsion of channel complexes is observed within Hector-3D (Figure 14). During the waxing cycle of channel formation, erosion occurs until an equilibrium profile is reached with the paleo-slope [38]. As the channel complexes in Hector-3D exhibit less incision than in the Pipeline-3D survey, this suggests the paleo-slope in this region was lower, decreasing incision and allowing intra-channel deposition to occur. The following waxing cycle will then find the most efficient path downslope promoting meandering or avulsion from the previous channel path. The channel complexes present within this interval were weakly-confined basin floor conduits which underwent significant sediment bypass feeding into a deep-water axial trough or widespread basinal fans within the deep-water Taranaki Basin [37,40,41]. While deposited sediment are likely mud-rich, the bright spectral response of the overbank anomalies in Figure 10, combined with terminated high-amplitude reflection packages (HARPs), indicate these are likely sand-prone deposits. Moving up in time through the stratal slices, sediment waves are consistently present throughout the dataset until SS 1 and Upper Tt (Figure 14). Upper Tt is characterized by low-sinuosity gullies across the survey (Figure 14). Integrating observations made in Pipeline-3D on Upper Tt, this indicates progradation of the shelf-slope system with a waning sediment supply, placing the Hector-3D survey within the shelf-slope system. Little to no discontinuities are present on these surfaces outside of the gullies which indicates overbank sedimentation has ceased to occur. These observations correlate well with other regional studies of the late Miocene southern Taranaki Basin deep-water depositional system [39]. Figure 15 presents a depositional model for the Pipeline-3D and Hector-3D areas, utilizing a point-source

model after [42] being integrated with a complex, low-gradient slope geometry [40]. The shelf-slope system in this part of the Taranaki Basin likely exhibited localized gradient changes and depocenters caused by localized structural inversion [8,37].

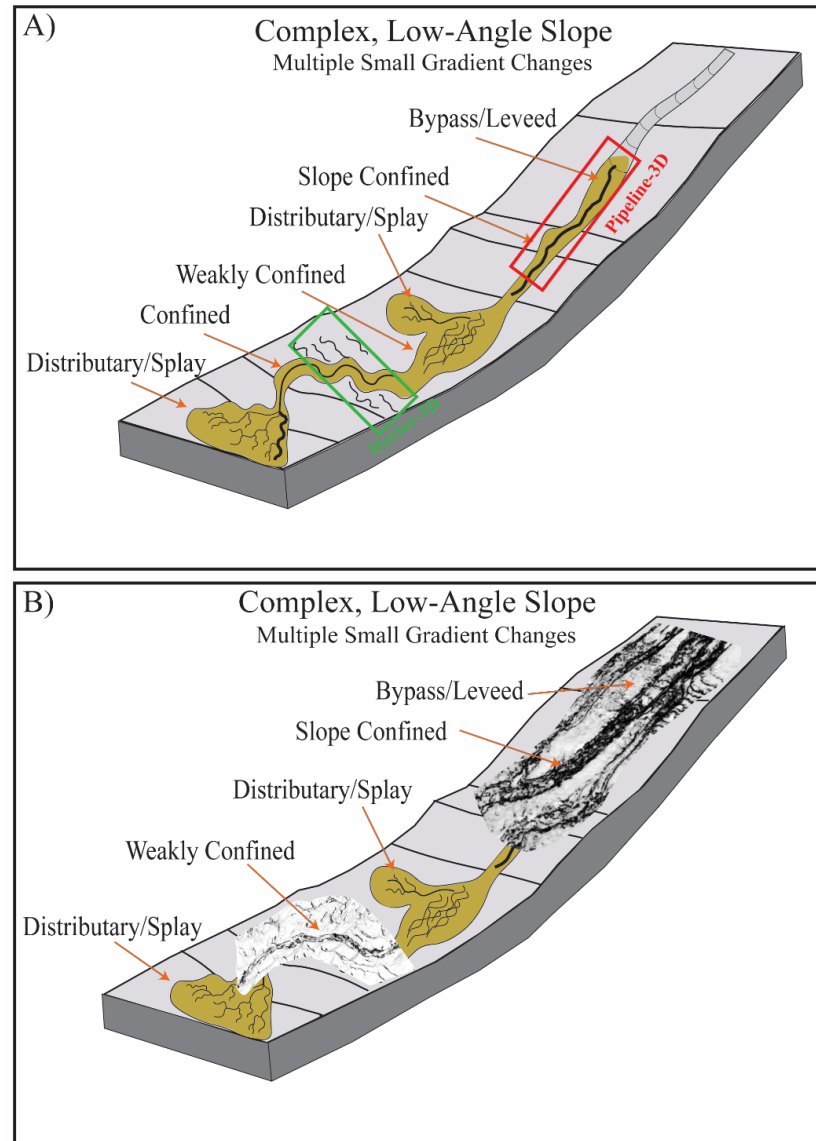


**Figure 15.** (A): Depositional model created for the region during the Lower Tt, modified after [40]. The red box corresponds to Pipeline-3D's area, while the green box represents the location of the Hector-3D area. (B): Depositional model with channels from both Pipeline-3D and Hector-3D study areas overlain.

## 6. Conclusions

Modern 3-D seismic attributes have allowed for the observation and analysis of key depositional elements of the southern equivalents of the late Miocene Mount Messenger Formation. The suite of seismic attributes used in this study provided valuable insight into the evolution and geometry of deep-water channel complexes. Energy ratio similarity and curvature excelled at illuminating the channel complexes' flanks and axes. Spectral decomposition also provided excellent visualization of the channel complexes, and in some cases, individual channels within the complexes.

The architecture of the channel systems in the Pipeline-3D area have characteristics of a slope-confined, middle-to-lower slope channel system, with frequently spaced channel complexes. The systems in Hector-3D resemble those of a weakly confined basin floor

distributary system in the lower Tt. During the large scale progradation which took place during the late Miocene through the Plio-Pleistocene, the observed incised valleys would have formed in response to regional crustal shortening associated with the initiation of the Southern Inversion Zone eastward. Sediment supplied from the erosion of the newly-uplifted South Island resulted in a large amount of transported sediment to the starved, subsiding basin along a slope with multiple small gradient changes. The internal architecture of channels varies in a way that matches those of erosional, slope-confined channel complexes and incision depth decreases from the proximal Pipeline-3D area to the distal Hector-3D area. This is likely caused by a decrease in the slope gradient combined with a decreasing sediment supply due to flow stripping and overbank deposition. The channel migration and wider complexes observed in the Hector-3D survey formed in response to the decreasing energy of the turbulent sediment flow, which match the characteristics of distributary channel systems basinward of the shelf-slope. The 3-D seismic surveys provide insight to the internal architecture of these late Miocene channel complexes in the Southern Taranaki Basin, as well as visualizing how multiple, frequently-spaced channel complexes transported eroded sediments basinward. The observed deepwater channel complexes in this study correlate, as the southern equivalents of the Mt. Messenger Formation, and deposition of the Mt. Messenger Formation was more widespread than previously known.

The base-of-slope component of the Mt. Messenger Formation equivalents observed in the Hector-3D survey suggests the best reservoir characteristics in this study area. The thick, high-amplitude reflectors observed within the wide sinuous channel complexes suggest coarse sand-prone deposits associated with coarser-grained sediments falling out of the turbidity current within the channel complex. The bright, lobate overbank deposits observed in spectral decomposition in Hector-3D could also serve as favorable reservoir targets. The shelf-slope component of the Mt. Messenger Formation equivalents displayed no favorable deposits and are interpreted to be composed of fine-grained mud rich sediments. While no hydrocarbons are present within the study interval, the insights gained from this study could be applied as an analogue elsewhere in the basin with a proven source.

**Author Contributions:** Conceptualization, C.S. and H.B.; methodology, C.S.; software, C.S.; validation, C.S. and H.B.; formal analysis, C.S.; investigation, C.S.; resources, H.B.; data curation, C.S. and H.B.; writing—original draft preparation, C.S.; writing—review and editing, H.B.; visualization, C.S.; supervision, H.B.; project administration, C.S. and H.B. funding acquisition, H.B. All authors have read and agreed to the published version of the manuscript.

**Funding:** This research was funded using start-up funds and undergraduate research award funds from the School of Geosciences at the University of Oklahoma, as well as funding from the Attribute Assisted Seismic Processing and Imaging (AASPI) consortium at the University of Oklahoma.

**Data Availability Statement:** Seismic and well data is available from New Zealand Petroleum and Minerals.

**Acknowledgments:** We would like to thank New Zealand Petroleum and Minerals for the seismic data used in this study. Additionally, we would like to thank Schlumberger for the donation of Petrel licenses. We would like to also thank Attribute Assisted Seismic Processing and Imaging (AASPI) consortium for providing the software to generate all attributes for this study.

**Conflicts of Interest:** The authors declare no conflict of interest. The funders had no role in the design of the study; in the collection, analyses, or interpretation of data; in the writing of the manuscript, or in the decision to publish the results.

## References

1. Browne, G.H.; Slatt, R.M. Outcrop and behind-outcrop characterization of a Late Miocene slope fan (channel-levee complex), Mt Messenger Formation, New Zealand. *Am. Assoc. Pet. Geol. Bull.* **2002**, *86*, 841–862.
2. King, P.R.; Browne, G.H.; Arnot, M.J.; Slatt, R.M.; Helle, K.; Stromsoy, I. A 2-D oblique-dip outcrop transect through an entire third-order, progradational, deep-water clastic succession (Late Miocene Mount Messenger-Urenui Formations), Taranaki Basin, New Zealand. *Atlas of deep-water outcrops. AAPG Stud. Geol.* **2007**, *56*, 238–240.

3. King, P.R.; Ilg, B.R.; Arnot, M.; Browne, G.H.; Strachan, L.J.; Crundwell, M.; Helle, K. Outcrop and Seismic Examples of Mass-Transport Deposits from a Late Miocene Deep-Water Succession, Taranaki Basin, New Zealand. *Mass-Transp. Depos. Deep. Settings* **2011**, *96*, 311–348. [[CrossRef](#)]
4. Baur, J.R.; King, P.R.; Stern, T.; Leitner, B. Development and Seismic Geomorphology of a Miocene Slope Channel Megasytem, Offshore Taranaki Basin, New Zealand. In *Seismic Imaging of Depositional and Geomorphic Systems: SEPM Foundation, Gulf Coast Section, 30th Annual Research Conference Proceedings*; SEPM Society for Sedimentary Geology: Tulsa, OK, USA, 2011; pp. 618–649. [[CrossRef](#)]
5. King, P.R.; Browne, G.H. Miocene turbidite reservoir systems in the Taranaki Basin. In *New Zealand: Established Plays and Analogues for Deep-Water Exploration: PESA Eastern Australasian Basins Symposium*; Positive Education Schools Association: Melbourne, VIC, Australia, 2001; pp. 129–139.
6. King, P.R.; Thrasher, G.P. *Cretaceous-Cenozoic Geology and Petroleum Systems of the Taranaki Basin, New Zealand*; Institute of Geological and Nuclear Sciences Monograph 13. 6 enclosures; Institute of Geological & Nuclear Sciences Limited: Lower Hutt, New Zealand, 1996; p. 243.
7. Browne, G.H.; King, P.R.; Higgs, K.E.; Slatt, R.M. Grain-size characteristics for Distinguishing Basin floor fan and slope Fan depositional settings: Outcrop and Subsurface examples from the late Miocene Mount Messenger Formation, New Zealand. *N. Z. J. Geol. Geophys.* **2005**, *48*, 213–227. [[CrossRef](#)]
8. Reilly, C.; Nicol, A.; Walsh, J.J.; Seebeck, H. Evolution of faulting and plate boundary deformation in the Southern Taranaki Basin, New Zealand. *Tectonophysics* **2015**, *651–652*, 1–18. [[CrossRef](#)]
9. Bull, S.; Nicol, A.; Strogen, D.; Kroeger, K.F.; Seebeck, H.S. Tectonic controls on Miocene sedimentation in the Southern Taranaki Basin and implications for New Zealand plate boundary deformation. *Basin Res.* **2019**, *31*, 253–273. [[CrossRef](#)]
10. Holt, W.E.; Stern, T.A. Subduction, platform subsidence, and foreland thrust loading: The late Tertiary development of Taranaki Basin, New Zealand. *Tectonics* **1994**, *13*, 1068–1092. [[CrossRef](#)]
11. Rotzien, J.R.; Browne, G.H.; King, P.R. Geochemical, petrographic, and uranium–lead geochronological evidence for multisourced polycyclic provenance of deep-water strata in a hybrid tectonic setting: The upper Miocene upper Mount Messenger Formation, Taranaki Basin, New Zealand. *AAPG Bull.* **2018**, *102*, 1763–1802. [[CrossRef](#)]
12. Arnot, M.J.; Bland, K.J.; Strogen, D.P.; Seebeck, H.C.; Bull, S.; Town, C.C.; Griffin, A.G.; Viskovic, G.P.D.; Hill, M.G.; Thrasher, G.; et al. *Atlas of Petroleum Prospectivity, Northwest Province: ArcGIS Geodatabase and Technical Report, GNS Science Data Series 23b 34 p. + 1 ArcGIS Geodatabase + 5 ArcGIS Projects, New Zealand*; GNS Science: Lower Hutt, New Zealand, 2016.
13. Strogen, D.P.; Bland, K.J.; Nicol, A.; King, P.R. Paleogeography of the Taranaki Basin region during the latest Eocene–Early Miocene and implications for the ‘total drowning’ of Zealandia. *N. Z. J. Geol. Geophys.* **2014**, *57*, 110–127. [[CrossRef](#)]
14. Laird, M.G.; Bradshaw, J.D. The Break-up of a Long-term Relationship: The Cretaceous Separation of New Zealand from Gondwana. *Gondwana Res.* **2004**, *7*, 273–286. [[CrossRef](#)]
15. Vonk, A.J.; Kamp, P.J.J. The Late Miocene Southern and Central Taranaki Inversion Phase (SCTIP) and related sequence stratigraphy and paleogeography. In *Proceedings of the 2008 New Zealand Petroleum Conference, Auckland, New Zealand, 9–12 March 2008*.
16. Hansen, R.J.; Kamp, P.J.J. Evolution of the Giant Foresets Formation, northern Taranaki Basin, New Zealand. In *Proceedings of the New Zealand Petroleum Conference, 24–27 February 2002*; Crown Minerals, Ministry of Economic Development: Wellington, New Zealand, 2002.
17. Strogen, D.P.; Bland, K.J.; Baur, J.R.; King, P.R.; Vonk, A.J.; Kamp, P.J.J. Neogene: Active margin tectonics. In *Updated Paleogeographic Maps for the Taranaki Basin and Surrounds*; GNS Science Report, 2011; Strogen, D.P., Compiler; GNS Science: Lower Hutt, New Zealand, 2010; pp. 36–60.
18. King, P.; Browne, G.; Slatt, R. *Sequence Architecture of Exposed Late Miocene Basin Floor Fan and Channel-Levee Complexes (Mount Messenger Formation), Taranaki Basin, New Zealand*; SEPM Society for Sedimentary Geology: Tulsa, OK, USA, 1994; Volume 15.
19. Browne, G.H.; Strachan, L.J.; King, P.R.; Malcolm, J.A. Mass-transport complexes from a late Miocene deep-water succession, Taranaki Basin, New Zealand: Scales, styles, and significance in relation to tectonic, eustatic, and autocyclic drivers. *Search Discov. Artic.* **2006**, 50040.
20. Rotzien, R.J.; Lowe, D.R.; King, P.R.; Browne, G.H. Stratigraphic architecture and evolution of a deep-water slope channel-levee and overbank apron: The Upper Miocene Upper Mount Messenger Formation, Taranaki Basin. *Mar. Pet. Geol.* **2014**, *52*, 22–41. [[CrossRef](#)]
21. Strong, C.P.; Wilson, G.J. *Taranaki Basin, New Zealand: Biostratigraphic Reassessment (Foraminifera and Dinoflagellates) of Key Western Platform Wells*; GNS Science Report 2002; GNS Science: Lower Hutt, New Zealand, 2002.
22. Roncaglia, L.; Fohrmann, M.; Milner, M.; Morgans, H.E.G.; Crundwell, M.P. *Well Log Stratigraphy in the Central and Southern Offshore Area of the Taranaki Basin, New Zealand*; GNS Science Report, 2013/27, 26p + enclosures; GNS Science: Lower Hutt, New Zealand, 2013.
23. Janocko, M.; Nemec, W.; Henriksen, S.; Warchoń, M. The diversity of deep-water sinuous channel belts and slope valley-fill complexes. *Mar. Pet. Geol.* **2013**, *41*, 7–34. [[CrossRef](#)]
24. Miall, A.D. *Architectural-Element Analysis: A New Method of Facies Analysis Applied to Fluvial Deposits*; Recognition of Fluvial Depositional Systems and Their Resource Potential; SEPM Society for Sedimentary Geology: Tulsa, OK, USA, 1985; pp. 33–81. [[CrossRef](#)]

25. Davies, R.J. *Seismic Geomorphology: Applications to Hydrocarbon Exploration and Production*; The Geological Society: London, UK, 2007.
26. Marfurt, K.J.; Kirilin, R.L.; Farmer, S.L.; Bahorich, M.S. 3-D seismic attributes using a semblance-based coherency algorithm. *Geophysics* **1998**, *63*, 1150–1165. [[CrossRef](#)]
27. Chopra, S.; Marfurt, K.J. Gleaning meaningful information from seismic attributes. *First Break* **2008**, *26*. [[CrossRef](#)]
28. Chopra, S.; Marfurt, K.J. Volumetric curvature attributes add value to 3D seismic data interpretation. *Lead. Edge* **2007**, *26*, 856–867. [[CrossRef](#)]
29. Partyka, G.; Gridley, J.; Lopez, J. Interpretational applications of spectral decomposition in reservoir characterization. *Lead. Edge* **1999**, *18*, 353–360. [[CrossRef](#)]
30. Laughlin, K.; Garossino, P.; Partyka, G. Spectral decomposition applied to 3D. *AAPG Explor.* **2002**, *23*, 28–31.
31. Li, F.; Qi, J.; Marfurt, K. Attribute mapping of variable-thickness incised valley-fill systems. *Lead. Edge* **2015**, *34*, 48–52. [[CrossRef](#)]
32. Silver, C.; Bedle, H. Overbank Sediment Waves in the Southern Taranaki Basin, New Zealand. *Interpretation* **2021**, *9*, C11–C15. [[CrossRef](#)]
33. Chenin, J.; Silver, C.; Bedle, H. Seismic geomorphology anomalies within a Pliocene deepwater channel complex in the Taranaki Basin, offshore New Zealand. *Interpretation* **2021**, *9*, C1–C10. [[CrossRef](#)]
34. Snedden, J.W. Channel-body basal scours: Observations from 3D seismic and importance for subsurface reservoir connectivity. *Mar. Pet. Geol.* **2013**, *39*, 150–163. [[CrossRef](#)]
35. Abreu, V.; Sullivan, M.; Pirmez, C.; Mohrig, D. Lateral accretion packages (LAPs): An important reservoir element in deep water sinuous channels. *Mar. Pet. Geol.* **2003**, *20*, 631–648. [[CrossRef](#)]
36. Posamentier, H.W. Depositional elements associated with a basin floor channel-levee system: Case study from the Gulf of Mexico. *Mar. Pet. Geol.* **2003**, *20*, 677–690. [[CrossRef](#)]
37. Baur, J.R. Regional Seismic Attribute Analysis and Tectono-stratigraphy of Offshore South-western Taranaki Basin, New Zealand. Ph.D. Thesis, Victoria University of Wellington, Wellington, New Zealand, 2012.
38. Kamp, P.J.; Green, P.F. Thermal and tectonic history of selected Taranaki Basin (New Zealand) wells assessed by apatite fission track analysis. *AAPG Bull.* **1990**, *74*, 1401–1419.
39. McHargue, T.; Pyrcz, M.J.; Sullivan, M.D.; Clark, J.D.; Fildani, A.; Romans, B.W.; Covault, J.A.; Posamentier, H.W.; Drinkwater, N.J. Architecture of turbidite channel systems on the continental slope: Patterns and predictions. *Mar. Pet. Geol.* **2011**, *28*, 728–743. [[CrossRef](#)]
40. Sprague, A.R.; Sullivan, M.D.; Champion, K.M.; Jensen, G.N.; Goulding, F.J.; Garfield, T.R.; Sickafoose, D.K.; Rossen, C.; Jennette, D.C.; Beaubouef, R.T.; et al. The physical stratigraphy of deep-water strata: A hierarchical approach to the analysis of genetically-related stratigraphic elements for improved reservoir prediction. In Proceedings of the AAPG Annual Meeting, Houston, TX, USA, 10–13 March 2002; pp. 10–13.
41. Bouma, A.H. *Key Controls on the Characteristics of Turbidite Systems*; Special Publications; Geological Society: London, UK, 2004; Volume 222, pp. 9–22. [[CrossRef](#)]
42. Reading, H.G.; Richards, M. Turbidite Systems in Deep-Water Basin Margins Classified by Grain Size and Feeder System. *AAPG Bull.* **1994**, *78*, 792–822. [[CrossRef](#)]